THE EUROPEAN
PHYSICAL JOURNAL A

Diverse mechanisms in proton knockout reactions from the Borromean nucleus ^{17}Ne

F. Wamers[1], C. Lehr[2], J. Marganiec-Gałazka[2,18], F. Aksouh[1,19], Yu. Aksyutina[1], H. Alvarez-Pol[3], L. Atar[2], T. Aumann[1,2], S. Beceiro-Novo[3,20], C. A. Bertulani[4], K. Boretzky[1], M. J. G. Borge[5], C. Caesar[1,2], M. Chartier[6], A. Chatillon[1], L. V. Chulkov[1,7], D. Cortina-Gil[3], P. Díaz Fernández[3,8], H. Emling[1], O. Ershova[1,9], L. M. Fraile[10], H. O. U. Fynbo[11], D. Galaviz[5], H. Geissel[1], M. Heil[1], M. Holl[8], H. T. Johansson[8], B. Jonson[8,a], C. Karagiannis[1], O. A. Kiselev[1], J. V. Kratz[12], R. Kulessa[13], N. Kurz[1], C. Langer[1,9], M. Lantz[8,14], T. Le Bleis[1,15], R. Lemmon[16], Yu. A. Litvinov[1], K. Mahata[1,17], C. Müntz[9], T. Nilsson[8], C. Nociforo[1], W. Ott[1], V. Panin[1,2], S. Paschalis[1,6], A. Perea[5], R. Plag[1,9], R. Reifarth[1,9], A. Richter[2], K. Riisager[11], C. Rodriguez-Tajes[3], D. Rossi[1,2], D. Savran[1], H. Scheit[2], G. Schrieder[2], P. Schrock[2], H. Simon[1], J. Stroth[9], K. Sümmerer[1], O. Tengblad[5], H. Weick[1], C. Wimmer[1,9]

[1] GSI Helmholtzzentrum für Schwerionenforschung GmbH, 64291 Darmstadt, Germany
[2] Institut für Kernphysik, Technische Universität Darmstadt, 64289 Darmstadt, Germany
[3] Instituto Galego de Física de Altas Enerxias, Universidade de Santiago de Compostela, E-15782 Santiago de Compostela, Spain
[4] Department of Physics and Astronomy, Texas A&M University-Commerce, Commerce, TX 75429, USA
[5] Instituto de Estructura de la Materia, CSIC, ES–28006 Madrid, Spain
[6] Department of Physics, University of Liverpool, Liverpool L69 3BX, UK
[7] NRC Kurchatov Institute, 123182 Moscow, Russia
[8] Institutionen för Fysik, Chalmers Tekniska Högskola, 41296 Göteborg, Sweden
[9] Institut für Angewandte Physik, Goethe Universität, 60438 Frankfurt am Main, Germany
[10] Grupo de Física Nuclear and IPARCOS, Universidad Complutense de Madrid, CEI Moncloa, E-28040 Madrid, Spain
[11] Department of Physics and Astronomy, University of Aarhus, 8000 Aarhus, Denmark
[12] Institut für Kernchemie Johannes Gutenberg-Universität Mainz, 55122 Mainz, Germany
[13] Instytut Fizyki, Uniwersytet Jagelloński, 30-059 Kraków, Poland
[14] Institutionen för fysik och astronomi, Uppsala Universitet, 751 20 Uppsala, Sweden
[15] Physik-Department E12, Technische Universität München, 85748 Garching, Germany
[16] Nuclear Physics Group, STFC Daresbury Lab, Warrington WA4 4AD, Cheshire, UK
[17] Nuclear Physics Division, Bhabha Atomic Research Centre, Trombay, Mumbai 400085, India
[18] Present Address: National Centre for Nuclear Research, Radioisotope Centre POLATOM, Andrzeja Sołtana 7, 05-400 Otwock, Poland
[19] Present Address: Department of Physics and Astronomy, College of Science, King Saud University, P.O. Box 2455, 11451 Riyadh, Kingdom of Saudi Arabia
[20] Present Address: National Superconducting Cyclotron Laboratory, MSU, East Lansing, MI 48824, USA

Abstract Nucleon knockout experiments using beryllium or carbon targets reveal a strong dependence of the quenching factors, i.e., the ratio (R_s) of theoretical to the experimental spectroscopic factors (C^2S), on the proton-neutron asymmetry in the nucleus under study. However, this dependence is greatly reduced when a hydrogen target is used. To understand this phenomenon, exclusive ^{1}H(^{17}Ne, 2p ^{16}F) and inclusive ^{12}C(^{17}Ne, 2p ^{16}F)X, ^{12}C(^{17}Ne, ^{16}F)X as well as ^{1}H(^{17}Ne, ^{16}F)X (X-denotes undetected reaction products) reactions with ^{16}F in the ground and excited states were anal- ysed. The longitudinal momentum distribution of ^{16}F and the correlations between the detached protons were studied. In the case of the carbon target, there is a significant devia- tion from the predictions of the eikonal model. The eikonal approximation was used to extract spectroscopic factor val- ues C^2S. The experimental C^2S value obtained with C target is markedly lower than that for H target. This is interpreted as rescattering due to simultaneous nucleon knockout from both reaction partners, ^{17}Ne and ^{12}C.

W. Ott: Deceased.

[a] e-mail: bjorn.jonson@chalmers.se (corresponding author)

Springer

1 Introduction

In the past half century, there has been a rapid development of experimental studies of atomic nuclei at various experimental facilities erected at accelerator laboratories worldwide. Long chains of isotopes of most of the chemical elements have been produced and studied in different dedicated experimental setups. A major step forward was made with the advent of production of beams of radioactive isotopes and, maybe even more, by the realisation of the strength of studies in inverse kinematics [1], which allow studying very short-lived nuclei. This article is the fourth in a series based on a novel technique for studying proton knockout reactions, with simultaneous measurements of the outgoing pair of protons and fragment [2–4]. After studying reactions with ^{12}C beams impinging on H and C targets, we here turn to the lightest bound isotope of the chemical element neon, ^{17}Ne, which has a two-proton separation energy of $S_{2p} = 933$ keV. Since its binary subsystems, the diproton and the resonant nucleus ^{16}F, are unbound, this is an example of a Borromean nucleus.

In the first part of the paper, we present relative energy spectra of ^{15}O + p and cross sections to the four resonances in ^{16}F, stemming from coupling of the $I^\pi = 1/2^-$ ground state of ^{15}O to s- and d- protons. Here we use the concept of spectroscopic factors (C^2S), which are phenomenological quantities used to describe the structure of a nucleus, the nature and filling of orbits by nucleons. Experimental C^2S's are mainly determined in nucleon knockout reactions using inverse kinematics, in which the nucleus under study bombards a target.

Nucleon knockout reactions induced by beryllium or carbon targets are the most commonly used reactions. The measured nuclear removal cross-section was interpreted as the sum of two contributions: (i) inelastic breakup, where the removed nucleon is absorbed by the target (also called stripping or knockout) and (ii) elastic breakup (also called diffraction dissociation) [5–13]. The assumption about absorption by the target was made despite the fact that the fate of the ejected nucleon was not traced either in the experiments or in the theoretical models used in the analysis of the experimental data. The extracted quenching factors (R_s) obtained using carbon or beryllium targets are consistent and do not show any obvious energy dependence over a wide range of energies, from 43 to 2100 MeV/u [14]. The main conclusion is that the obtained R_s values greatly depend on the proton-neutron asymmetry. However, this strongly contradicts the nucleon knockout reactions on hydrogen targets and nucleon transfer reactions (see, e.g., section 7, Fig. 56 in Ref. [15]).

The first measurements, in which the residue was detected in coincidence with a fast proton following the one-proton knockout reactions, ^{9}Be(^{9}C, p ^{8}B)X and ^{9}Be(^{8}B, p ^{7}Be)X, at beam energies slightly below 100 MeV/u, were performed at the National Superconducting Cyclotron Laboratory [16]. The data obtained in this experiment revealed that the knocked-out nucleon is not absorbed in the Be target.

Another pioneering experiment was performed at GSI Helmholtzzentrum für Schwerionenforschung using triple coincidences between the residue and protons ejected from the projectile and from the target: ^{1}H(^{12}C, 2p ^{11}B) [2] and ^{12}C(^{12}C, 2p ^{11}B)X [3]. The experiment with the carbon target showed that in 61(5)% of the cases, the knocking out of a nucleon from the projectile is accompanied by the simultaneous knocking out of a nucleon from the target. Such a secondary interaction of nucleons knocked-out from the target can lead to the destruction of the residue nucleus. However, the spectroscopic factors obtained from the experimental cross sections, using the standard eikonal approximation, remain the same within the statistical uncertainties, $C^2S = 2.80(12)$ for the carbon [3] and $C^2S = 2.58(30)$ for the hydrogen [2] target. Thus, in the case of a strongly bound ^{12}C projectile, the nucleons stripped from the C target have an insignificant effect on the cross section.

The aim of the present paper is to extend this analysis to the case where a relativistic beam of the weakly bound two-proton halo nucleus ^{17}Ne impinges on both a carbon and hydrogen target. The results of this experiment with a beam incident on a hydrogen target are given in [4], where the emphasis is on the structure of the two-proton halo in ^{17}Ne. Now, the main attention is paid to the diversities in the mechanisms of proton knockout on different targets.

The choice of ^{17}Ne to study the difference in reaction mechanisms induced by different targets is made due to the halo structure of its ground state. The ^{15}O+p+p models give consistent results in describing the overall features of the ^{17}Ne ground state, such as matter radii, charge radii, density distribution [17–19]. The quenching of spectroscopic factors is considered as an effect of short range nucleon-nucleon correlations. The halo protons are free from this effect. The two external protons are in a mixed configuration and occupy $1s_{1/2}$ and $0d_{5/2}$ shells. This provides an additional opportunity to check whether the ratio $\sigma(1s)/\sigma(0d_{5/2})$ is independent of the target.

2 Experimental setup

The details of the experiment setup used here have been described in our earlier papers [2,4]. A primary ^{20}Ne 630 MeV/u beam from the SIS-18 synchrotron at GSI was directed towards a reaction target, and a secondary ^{17}Ne beam of 500 MeV/u was selected in the FRS fragment separator. This beam impinged onto, either a 370 mg/cm^2 C target or a 213 mg/cm^2 CH$_2$ target, where the C target both served as a dedicated target, and was used to extract the reaction contribution of the hydrogen component in the CH$_2$ target.
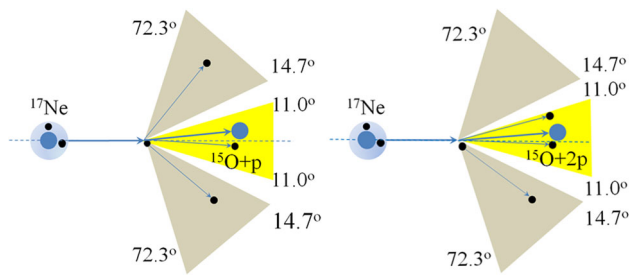
Fig. 1 Schematic illustration of the two types of reactions with a ^{17}Ne beam on a hydrogen target. **i** Proton knockout from a proton halo (left). **ii** Excitation of ^{17}Ne, leading to the formation of ^{15}O and two protons (right). The angular regions covered by the two detector complexes, at small angles and at large angles, are shown in yellow and beige coloured shadows. The proton knockout reaction channel is obtained by requiring either two protons in the Crystal Ball or one proton at small angles

Measurements with an empty target allowed a determination of the level of background from the surrounding material.

The six double-sided silicon strip detectors (DSSSD) located around the target are of particular importance in the analysis presented here. Four of them, forming an open box just behind the target, are surrounded by a spherical detector, the Crystal Ball (CB), consisting of 162 NaI(Tl) crystals. The CB detector, covers polar angles from 14.7° to 72.3°. This eliminates diffraction dissociation events, which are focused at smaller angles. This combination of detectors allowed for the detection of the azimuth ($\varphi_{1(2)}$) and polar ($\vartheta_{1(2)}$) angles of the knocked-out protons. Measurements of γ rays reveal de-excitation of excited states in ^{15}O.

Two other DSSSD's are located behind the target, covering a polar angular range of $0° \leq \vartheta \leq 11°$ for both fragments and protons. Behind the dispersing ALADIN dipole magnet, the fragments could additionally be detected in two scintillation fiber-trackers, and protons in two drift chambers. Time-of-flight walls, consisting of plastic scintillators, were used to detect fragments and protons with an almost 100 % detection efficiency for both. The requirement of a proton multiplicity equal to unity in this range of polar angles also led to an elimination of the diffraction dissociation component (see Fig. 1).

Two sources of background have been considered: (i) reactions stemming from the beam interacting with materials outside the target, which was determined in an empty target run, (ii) reactions with excitation of bound states in ^{15}O, which decay by γ-ray emission.

All experimental data were corrected for geometrical acceptance and detection efficiency. The given uncertainties are statistical. Systematic errors, due to uncertainties in target thickness and detection efficiencies of the protons and the ^{15}O fragments, are of the order 2–3%. In the case when 2p detection in the Crystal Ball is required, the systematic uncertainty of the proton detection efficiency is about 6% [20,21].

3 Relative-energy spectra

Measurements with the required $p_{mult} = 2$ (i.e., detecting ^{15}O plus two protons at forward angles as shown in Fig. 1(right)) [22] yielded a relative energy spectrum for the ^{15}O + 2p system which shows a broad distribution with a maximum at about 4–5 MeV and several peaks at positions of excited states in ^{17}Ne (see Fig. 7 in Ref. [22]). The spectrum represents the diffraction dissociation of ^{17}Ne plus the excitation and decay of the ^{17}Ne states. These reaction channels were excluded in the present experiment by the request $p_{mult} = 1$. The relative energy spectrum for the ^{15}O + p system, calculated by Eq. 1 is the basic experimental quantity in the present analysis.

$$E_{fp} = |\mathbf{P}_f + \mathbf{P}_p| - M_f - m_p, \tag{1}$$

with c = 1 and where $\mathbf{P}_f$ ($\mathbf{P}_p$) and M_f (m_p) are the ^{15}O (p) four-momenta and masses, respectively.

The experimental $d\sigma/dE_{fp}$ spectra obtained with $p_{mult} = 1$ are shown in Fig. 2 for the H target and in Fig. 3 for the C target. The elimination of diffraction dissociation can be achieved in two ways, either by detecting the knocked out and the recoiled proton in the CB detector, or by requiring a proton multiplicity of $p_{mult} = 1$ in the forward-angle detectors. But when measuring with a C-target, only the second method can be used. The relative energy spectra for the H target, are shown in Fig. 2a and b. A slight reduction of the cross sections is seen for the latter, but still within the experimental uncertainty. The fact that the sum of the spectroscopic factors in both cases are close to two, as expected for a two-proton halo, shows the validity of the method. In the case of C target, the spectroscopic factor can only be obtained by requiring $p_{mult} = 1$, as shown in Fig. 3a. Measurements with additional registration of two protons in the CB have shown that proton disruption from the target nucleus cannot be neglected, as shown in Fig. 3b.

In this experiment, only coincidences with protons were used. However, the cross-sections in Fig. 3b, as well as in Table 1 for the C target, additionally take into account the contribution of neutron knockout from the target by using the ratio of total cross-sections $R_{n/p} = \sigma_{np}/\sigma_{pp} = 1.09$ for a proton energy of 500 MeV [23]. This $R_{n/p}$ value is close to the experimental ratio $R_{n/p} = 1.06(13)$ obtained in ^{12}C(^{12}C, 2p ^{11}B) and ^{12}C(^{12}C, pn ^{11}B) at 398 MeV/u [3].

The resonances in the experimental spectra were analysed, assuming Breit-Wigner shaped resonances with energy-dependent resonance widths. The contributions of the Coulomb forces were taken into account by using ^{15}O-p regular and irregular Coulomb wave functions. The fitting functions were smoothed by the R3B/LAND detectors response obtained by Monte Carlo simulation using R3BRoot [24]. The integrals
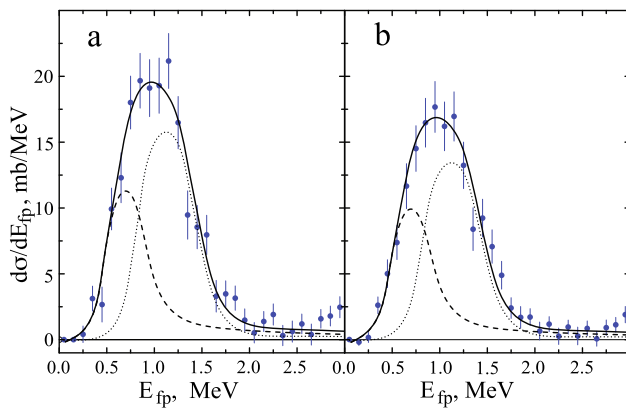
Fig. 2 Relative energy spectra in ^{15}O+p after knocking out a proton from ^{17}Ne in a H target. The curves show the results of a fit to the data using Breit-Wigner shaped resonances. **a** Data obtained by registering only the proton and ^{15}O fragment, which are the decay products of ^{16}F ($\chi^2/N = 1.21$). **b** Measurements were made with additional registration of two protons in CB ($\chi^2/N = 0.79$)
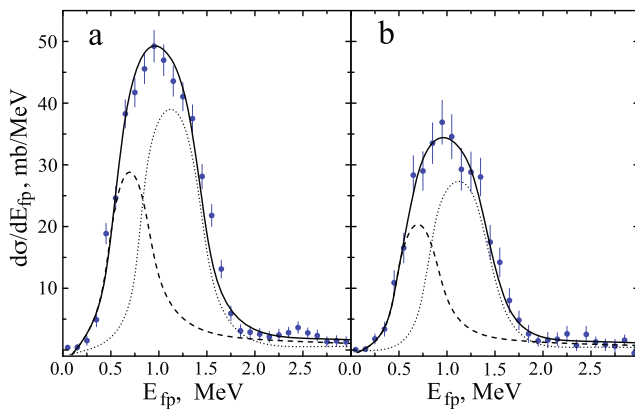
Fig. 3 Relative energy spectra in ^{15}O + p after knocking out a proton from ^{17}Ne in a C target. The curves show the results of a fit using Breit-Wigner shaped resonances. **a** Data obtained by registering only the proton and ^{15}O fragment, which are the decay products of ^{16}F ($\chi^2/N = 1.65$). **b** Measurements were made with additional registration of two protons in CB ($\chi^2/N = 0.69$)

of fitting function in the region $0 \leq E_{fp} \leq 10$ MeV were normalised to unity.

Four resonances are known in the energy region $0 < E_{fn} < 2$ MeV: ^{16}F(0^-) and ^{16}F(1^-), populated after proton knock-out from the $1s$ shell, and ^{16}F(2^-) and ^{16}F(3^-) populated after proton knockout from the $0d_{5/2}$ shell. The positions and widths of these four resonances were taken from Ref. [25] and kept fixed during the fitting procedure. Only the cross sections $\sigma_{01} = \sigma(0^-) + \sigma(1^-)$, $\sigma_{23} = \sigma(2^-) + \sigma(3^-)$ were used as fitting parameters. The ratios of the cross-sections $\sigma(0^-)/\sigma(1^-)$ and $\sigma(2^-)/\sigma(3^-)$ were assumed to be $2I + 1$ ratios, as was used for the ^{16}F resonant states in Ref. [26]. In the case of the C target, with the requirement of 2p detected in the CB, only the total cross-sections $\sigma_{01} + \sigma_{23}$ were used as fitting parameters with the same ratio σ_{01}/σ_{23} as in the case

without CB. The resulting ratio of cross sections with and without 2p detection in the CB can be interpreted in such a way that proton knockout from ^{17}Ne is accompanied by nucleon ejection from the C target for 69.8(23)% of events. Note, that knocking out an α-particle can also be a significant process.

Fitting of the energy spectra was performed using MINUIT, a system for function minimisation and analysis of the parameter errors and correlations [27]. The results from the fits are given in Table 1. The key quantity in the interpretation of the experimental cross sections are the calculated single-particle cross sections σ_{sp}, corresponding to one proton on the shell. [1]

The calculation of σ_{sp} was performed to describe the knockout of one proton from ^{17}Ne under the assumption that ^{16}F remains in a resonant state that decays with the emission of a proton. The eikonal formalisms described in Ref. [28] and Ref. [29,30] were used for hydrogen and carbon targets, respectively.

The single-particle wave functions of a bound state were obtained using the nuclear potential with a Woods-Saxon shape plus a spin-orbit interaction, reproducing the effective binding energy of the nucleon. The potential parameters were the same in both calculations. The matter density parameters for ^{17}Ne and ^{12}C were based on systematics of experimental data given in Ref. [31]. The same density distribution for ^{17}Ne was used in both calculations. The calculation of the elastic scattering amplitudes using the eikonal wave functions was based on the parameterization of the elastic scattering nucleon-nucleon cross-sections given in Ref. [23]. In both cases, the modification of the interaction of colliding protons in nuclear matter was taken into account. The (p, 2p) reaction model [28] explicitly takes into account the absorption of the incoming and outgoing proton due to multiple scattering effects inside ^{17}Ne. The possibility of nucleons being knocked out of the target nucleus was not considered. The calculated cross sections and the obtained spectroscopic factors are given in Table 1.

The sum of spectroscopic factors obtained in the ^{1}H(^{17}Ne, ^{15}O + p) reaction is 2.08(10), whereas in the ^{12}C(^{17}Ne, ^{15}O + p) reaction it is 1.502(35), which is 28(5)% less. The reason for the decrease in the value of the spectroscopic factor could be dissipative mechanisms acting in the final state of the reaction products. Signs of such processes can be observed in the longitudinal momentum distribution of the remnant nucleus and in correlations between detached nucleons.

---

[1] The σ_{sp} values serve to convert the measured partial cross sections to experimental spectroscopic factors $C^2S = \sigma_{exp}/\sigma_{sp}$. With this definition, C^2S can be interpreted as the effective number of nucleons in an orbit.

Table 1 Cross sections for population of resonances in ^{16}F $\sigma(0^-)+\sigma(1^-)$ and $\sigma(2^-)+\sigma(3^-)$, theoretical single-particle cross sections σ_{sp} and spectroscopic factors C^2S for $^{15}O \otimes \pi(1s)^2$ and $^{15}O \otimes \pi(0d_{5/2})^2$ configurations in ^{17}Ne(g.s)

Mode	Resonances	σ_{exp} mb	σ_{sp} mb	C^2S
Hydrogen target				
$p_{mult} = 1$	$^{16}F(0^-, 1^-)$	8.61 (77)	11.65	0.739 (66)
	$^{16}F(2^-, 3^-)$	12.30 (76)	9.16	1.343 (83)
	Sum of C^2S			2.08 (10)
2p in CB	$^{16}F(0^-, 1^-)$	7.63 (65)	11.65	0.655 (56)
	$^{16}F(2^-, 3^-)$	10.54 (67)	9.16	1.151(73)
	Sum of C^2S			1.806 (92)
Carbon target				
$p_{mult} = 1$	$^{16}F(0^-, 1^-)$	22.73 (91)	46.06	0.493 (20)
	$^{16}F(2^-, 3^-)$	31.10 (90)	30.80	1.009 (29)
	Sum of C^2S			1.502 (35)
2p in CB	$^{16}F(0^-, 1^-)$	15.86 (82)	No theoretical	
	$^{16}F(2^-, 3^-)$	21.71 (95)	description yet	

4 Longitudinal-momentum distributions

The analysis of the longitudinal-momentum distribution for ^{16}F was used to check the applicability of the eikonal theory. It has been noted [29] that the longitudinal distribution of the remnant gives the most direct information about single-particle properties, since it is insensitive to collision details and target size, in contrast to the transverse distribution, which is distorted by diffraction effects and Coulomb scattering. The maximum of the longitudinal distribution is observed at 17.310(50) GeV/c corresponding to 495.9(2.3) MeV/u for the ^{16}F energy. This value is, within statistical errors, equal to the projectile energy after the target of 494.6 MeV/u. The calculated momentum distributions were used to describe the measured distributions, see Fig. 4a for the H target ($\chi^2/N = 32.4/33$) and Fig. 4b for carbon target ($\chi^2/N = 174/49$). In the χ^2 analysis [32], the p-value is the probability of getting χ^2 greater than that obtained in the fitting, and indicates whether the experimental data support the hypothesis being applied. The p-value is 0.5 for data acquired with the H target, but is $6.7 \cdot 10^{-16}$ for the C target. This indicates a strong violation of the eikonal approximation in the case of the C target. The eikonal model predicts a symmetric distribution of the longitudinal momentum.

An asymmetry in the longitudinal momentum distribution is observed in many experiments, but only for complex (non-hydrogen) targets and for beam energies below 100 MeV/u [33–39]. Such asymmetric distributions can arise in the case of diffraction dissociation of weakly bound systems [34] or, when the projectile energy per nucleon is comparable in magnitude to the nucleon separation energy, due to the interaction of the emitted nucleon with the target in the final state
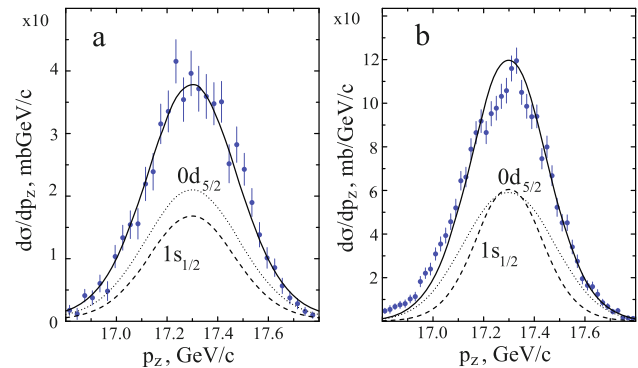

Fig. 4 Longitudinal-momentum distributions for ^{16}F: **a** from the hydrogen target and **b** from the carbon target. The momentum distributions were obtained in the energy window $0 < E_{fp} < 2$. The results of the fitting are shown as smooth lines ($\chi^2/N = 0.98$ for (**a**) and $\chi^2/N = 3.55$ for (**b**))

[39]. Asymmetry in the longitudinal momentum distribution at 500 MeV/u beam energy with detected events only from the knockout reaction is observed for the first time. The ejection of nucleons from the target with a relative intensity of $\approx 70\%$ can be the cause of the asymmetry in the longitudinal momentum distribution. However, the effects of target fragmentation, which can significantly change the derived spectroscopic factors, have not yet been taken into account in theoretical models.

5 Correlations between protons stripped from projectile and target nuclei

Additional information on the reaction mechanisms was obtained by comparing the correlations between the proton
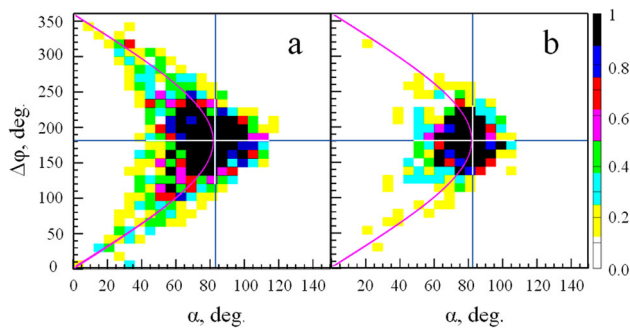
Fig. 5 Density of registered events, depending on the angle between the momentum vectors of protons registered in the Crystal Ball (α) and the difference in their azimuthal angles ($\Delta\varphi = |\varphi_1 - \varphi_2|$). **a** ^{12}C(^{17}Ne, 2p), **b** ^{1}H(^{17}Ne, 2p). The density is given in arbitrary units. The distributions are normalised to the same integral. The red curves are drawn using Eq. 2 and assuming $\vartheta_1 = \vartheta_2 = 41.6°$. The right-hand colour scale shows the density of events in relative units

knocked out of ^{17}Ne and the recoil proton from H target with the correlations between protons knocked out simultaneously from ^{17}Ne and C target. The density of registered events as a function of opening angle and the difference in their azimuthal angles ($\Delta\varphi = |\varphi_1 - \varphi_2|$) are shown in Fig. 5a and b for the C and H targets, respectively. The opening angle (α), i.e. the angle between the directions of flight of the two protons, was calculated from:

$$\cos\alpha = \sin\vartheta_1 \sin\vartheta_2 \cos\Delta\varphi + \cos\vartheta_1 \cos\vartheta_2 \qquad (2)$$

The two-dimensional distributions in Fig. 5 show a maximum at $\alpha = 83.2°$ and $\Delta\varphi = 180°$. This coincides with the position of the maximum in $d\sigma/d\alpha$ for elastic scattering of protons at an energy of 500 MeV in the laboratory system (see Appendix). A characteristic feature of the two-dimensional distribution in Fig. 5a is the wings that are spreading out from $\alpha = 83.2°$ and $\Delta\varphi = 180°$ in two directions $\Delta\varphi = 0°$ and $\Delta\varphi = 360°$ towards $\alpha = 0°$. The wings extend along the curve calculated by using Eq. 2 with $\vartheta_1 = \vartheta_2 = 41.6°$. Thus, in the case of a C target, there is a probability that both knocked-out nucleons fly almost in the same direction, close to 40° relative to the beam.

According to Eq. 2, the appearance of the wings could be naturally explained as an effect of poor experimental resolution of the azimuth angle. However, the wings are essentially absent for the H target, as can be seen in Fig. 5b, which rules out such a simple explanation, since the $\Delta\varphi$ resolution is the same for both targets. Another explanation for the wings could be that they are a consequence of internal momentum distribution of nucleons in the target nucleus, but the equality of the angles $\vartheta_1 \approx \vartheta_2$, combined with certain probability that both protons are flying in the same direction, needs to be explained. The interaction of reaction products in the final state can also be considered as a possible cause.

The wings effect can reduce the survivability of the ^{15}O core due to rescattering of both stripped protons inside the nuclear matter of the projectile and, therefore, reduce the spectroscopic factor. Finding an explanation for the observed phenomenon is a challenging task.

6 Summary

In summary, we have investigated the mechanism of the single proton removal from ^{17}Ne in the different reactions by selecting only the one-proton knockout component: ^{12}C(^{17}Ne, ^{16}F)X, ^{12}C(^{17}Ne, 2p ^{16}F)X and ^{1}H(^{17}Ne, 2p ^{16}F). The experiment shows that the mechanism of knocking out a valence proton from ^{17}Ne incident on a carbon target leads to simultaneous nucleon knockout from the target with a 70% probability.

Unexpected is the effect when both knocked-out nucleons fly, with a certain probability, in the same direction, increasing the importance of secondary processes in the projectile and thereby decreasing the probability of core-nucleus survival. The obtained spectroscopic factor of proton knockout from the ^{17}Ne proton on the H target is 2.08 (10). Within statistical uncertainty, this is equal to 2, as expected for a nucleus with a two-proton halo. However, this value decreases to 1.502 (35) for the C target, which indicates the importance of accounting for nucleons knocked-out of the target in the theoretical description of the process. The existing computer codes use nucleon-nucleon cross sections and experimental values of the density parameters. The cluster structure of the target nucleus is not taken into account.

Let us finally make some remarks about the importance of these results for experiments at future facilities with ultra-relativistic ion-beam energies. It is clearly demonstrated that in complex target reactions, the interaction between nucleons in the beam and target perturbs the reliability of structure information. Modern developments of technique of making pure H targets is very advanced today. This, together with existing theory [28], makes us believe that in future experiments like QFS, hydrogen will certainly be the target material of choice. However, the very understanding consequences of simultaneous knocking nucleons out of a projectile and out of a complex target is also an attractive and important goal.

7 Appendix

It is interesting to compare the proton-proton correlations after proton knockout from the ^{17}Ne proton halo with the correlations in elastic scattering of protons in the laboratory coordinate system. The differential cross section in the center-of-mass system at an energy of about 500 MeV is close to isotropic [40], and the calculations shown in Fig. 6 were performed assuming an isotropic cross section. Figure 6a displays ϑ_1 as function of ϑ_2. The non-relativistic case is shown as a dotted line. The greatest deviation from non-relativistic calculations is observed at $\vartheta_1 = \vartheta_2 = 41.6°$. In the case of proton-proton scattering, the angle between flight direction of scattered and recoiled protons $\alpha = \vartheta_1 + \vartheta_2$ while difference in azimuth angles $\Delta\varphi = \varphi_1 - \varphi_2$ is equal to 180°. The maximum in $d\sigma/d\alpha$ goes to infinity at $\alpha = 83.2°$, where the scattering angles are equal, as shown in Fig. 6b. Such coequality of angles at $\Delta\varphi = 180°$ is observed in the experiment when a proton is knocked-out of the halo (see solid lines in Fig. 5a, b).
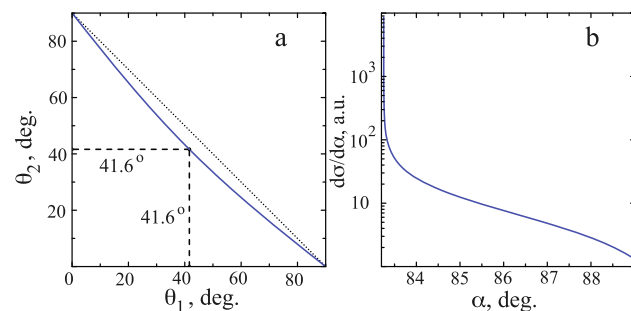
Fig. 6 Correlations between recoil and scattered protons in elastic proton-proton scattering. **a** The dependence of the emission angle of one proton on the emission angle of another proton. The result for non-relativistic kinematics is shown as a dotted line. **b** Differential cross section of elastic scattering $d\sigma/d\alpha$ as a function of the angle between the flight directions of protons α. $d\sigma/d\alpha$ goes to infinity at $\alpha = 83.2°$

References

1. C. Fahlander, B. Jonson (Eds.), Phys. Scr. T **152**, 010301 (2013)
2. V. Panin et al., Phys. Lett. B **753**, 204 (2016)
3. V. Panin et al., Phys. Lett. B **797**, 134802 (2019)
4. C. Lehr et al., Phys. Lett. B **827**, 136957 (2022)
5. M.S. Hussein, K.W. McVoy, Nucl. Phys. A **445**, 124 (1985)
6. A. Navin et al., Phys. Rev. Lett. **85**, 266 (2000)
7. J. Tostevin, Nucl. Phys. A **682**, 320 (2001)
8. V. Maddalena et al., Phys. Rev. C **63**, 024613 (2001)
9. B.A. Brown, P.G. Hansen, B.M. Sherrill, J.A. Tostevin, Phys. Rev. C **65**, 061601 (2002)
10. P.G. Hansen, J. Tostevin, Ann. Rev. Nucl. Part. Sci. **53**, 219 (2003)
11. Y.Z. Sun et al., Phys. Rev. C **93**, 044607 (2016)
12. C. Hebborn, P. Capel, Phys. Rev. C **104**, 024616 (2021)
13. Y.Z. Sun et al., Phys. Rev. C **106**, 034614 (2022)
14. Y.-P. Xu, D.-Y. Pang, C.-X. Yuan, X.-Y. Yun, Chin. Phys. C **46**, 064102 (2022)
15. T. Aumann et al., Prog. Part. Nucl. Phys. **118**, 103847 (2021)
16. D. Bazin et al., Phys. Rev. Lett. B **102**, 232501 (2009)
17. J. Casal et al., Phys. Rev. C **94**, 054622 (2016)
18. S.-S. Zhang, E.-G. Zhao, S.-G. Zhou, Eur. Phys. J. A **49**, 77 (2013)
19. H.T. Fortune, R. Sherr, Phys. Lett. B **503**, 70 (2001)
20. L. Atar et al., Phys. Rev. Lett. **120**, 052501 (2018)
21. M. Holl et al., Phys. Lett. B **795**, 682 (2019)
22. F. Wamers et al., Phys. Rev. C **97**, 034612 (2018)
23. C.A. Bertulani, C. De Conti, Phys. Rev. C **81**, 064603 (2010)
24. D. Bertini, J. Phys: Conf. Ser. **331**, 03203 (2011)
25. I. Stefan et al., Phys. Rev. C **90**, 014307 (2014)
26. C.R. Hoffman, B.P. Kay, J.P. Schiffer, Phys. Rev. C **94**, 024330 (2016)
27. F. James, M. Roos, Comput. Phys. Comm. **10**, 343 (1975)
28. T. Aumann, C.A. Bertulani, J. Ryckebusch, Phys. Rev. C **88**, 064610 (2013)
29. C.A. Bertulani, P.G. Hansen, Phys. Rev. C **70**, 034609 (2004)
30. C. Bertulani, A. Gade, Comput. Phys. Comm. **175**, 372 (2006)
31. H. De Vries, C. De Jager, C. De Vries, At. Data Nucl. Data Tables **36**, 495 (1987)
32. p-value. Calculator for Chi-Square Distribution https://www.omnicalculator.com/statistics/p-value
33. T. Aumann et al., Phys. Rev. Lett. **84**, 35 (2000)
34. J.A. Tostevin et al., Phys. Rev. C **66**, 024607 (2002)
35. J. Enders et al., Phys. Rev. C **65**, 034318 (2002)
36. A. Gade et al., Phys. Rev. C **69**, 034311 (2004)
37. E. Sauvan et al., Phys. Rev. C **69**, 044603 (2004)
38. A. Gade et al., Phys. Rev. C **71**, 051301 (2005)
39. F. Flavigny et al., Phys. Rev. Lett. **108**, 252501 (2012)
40. G.W. Hoffmann et al., Phys. Rev. C **37**, 397 (1988)